

Article

Cavity-Assisted Spin-Orbit Coupling of Ultracold atoms

Lin Dong ¹, Chuanzhou Zhu ¹ and Han Pu ^{1*}

¹ Department of Physics and Astronomy, Rice Quantum Institute, Rice University, Houston, Texas, 77251-1892, USA

* Author to whom correspondence should be addressed; hpu@rice.edu

Received: xx / Accepted: xx / Published: xx

Abstract: We investigate dynamical and static properties of ultracold atoms confined in an optical cavity, where two photon Raman process induces effective coupling between atom's pseudo-spin and center-of-mass momentum. In the meantime, atomic dynamics exerts a back action to cavity photons. We adopt both mean field and master equation approach to tackle the problem and found surprising modifications to atomic dispersions and dynamical instabilities, arising from the intrinsic nonlinearity of the system. Correspondence between semi-classical and quantum limits is analyzed as well.

Keywords: cavity quantum electrodynamics; cold atoms; spin-orbit coupling

1. Introduction

Laser light is a versatile and standard experimental tool in the forefront field of modern quantum optics and ultracold atomic gases. Spatial coherence allows a laser beam to be focused to a tight spot and stay narrow over long distances. Extremely narrow energy spectrum, given by high temporal coherence, makes it ideal to create highly controllable and tunable optical potentials, when far red detuned from an atomic resonances. The pioneering experimental achievement of Bose-Einstein condensation (BEC) [1–3], and of Fermi degenerate dilute gases [4–6] has offered a plethora of opportunities to study quantum properties of light and ultracold matter. A major focus in recent years has been the exploration of quantum properties of many-body strongly correlated systems (for reviews, cf [7,8]), by trapping coherent matter waves in optical potentials, e.g. harmonic trap, optical lattices, etc. A high level of microscopic understanding sheds light on some of long sought problems in condensed matter and high

energy physics, e.g. Bose-Hubbard (BH) model [9,10], universal physics of strongly interacting fermions [11,12]. However, quantum effects of the light were widely neglected to a large extent. In both complex experimental setups and theoretical models, laser light is commonly treated as a classical auxiliary tool to prepare, probe and manipulate intriguing atomic states. Atom-field interaction can be well captured by the minimal-coupling Hamiltonian at the dipole approximation level. In the far red detuned limit, coherent scattering of photon dominate and the resulting dipole light force can be derived from the optical potential proportional to laser intensities due to Stark-shift.

The level playing field changes when atom is confined in high finesse optical cavity [13–15], where atom and the light field will mutually affect each other. This is simply because intra-cavity photon and atoms highly frequently scatter with each other due to the geometric confinement, the light field no longer serves as a conservative potential. Dipole force gets strongly enhanced and atom's back-action onto light gets significant. In general, this demands a self-consistent solution for both light and atom by treating them on equal footing. On the one hand, the quantum properties of atom will manifest themselves in the scattered light, which leads to novel technical advancements in light measurement of atomic states. On the other hand, the quantized light field imprints nontrivial marks on atomic many-body dynamics as well as equilibrium states. In this regard, cavity quantum electrodynamics (CQED) further enriches the picture of using quantum simulator to understand real world materials, [16–18].

Following the cornerstone of traditional CQED, where only internal dynamics of the atom is relevant in typical setups, we have witnessed important experimental progresses in putting ultracold atoms inside optical cavities. The center-of-mass (COM) motion of the atom gets non-negligible in this “ultracold atom + optical cavity” system, which has been extensively explored both experimentally [19–23] and theoretically [24,25].

Another branch of series breakthroughs in cold atom research originate in the realization of artificial (synthetic) gauge potentials for neutral atoms, first in bosonic systems [26,27] and later in fermionic counterparts [28,29]. Laser fields are properly aligned and designed in such a way that trapped atoms may mimic charged particles in a magnetic field with emergence of Lorentz-like force. The synthesis is achieved by inducing two-photon Raman transition between two hyperfine ground state. Using a group of degenerate (or quasi-degenerate) pseudospin eigenstates, non-abelian dynamics of cold atoms in light fields is generated, which effectively leads to the spin-orbit coupling (SOC) for cold atoms, simulating the one appearing for electrons in condensed matter. Synthetic SOC refers to the coupling between pseudospins (a.k.a. hyperfine states) and atom's COM, rather than the generic interaction between electron's spin (or magnetic moment) and angular momentum operator in quantum mechanics. SOC is essential in understanding numerous underlying condensed matter phenomena and nuclear particle physics [30], including *inter alia* topological insulators, Majorana and Weyl fermions, spin-Hall effects, etc [31–35].

Thus far, all the experimental realizations of synthetic SOC in quantum gases, utilize classical laser fields to assist Raman transition, which are not affected by atom's COM reciprocally. In this article of special issue, we first of all briefly review our previous work [36], and theoretically explore the full quantum treatment beyond semi-classical mean field formalism, then investigate the correspondences in quantum and semi-classical regions. We consider a single atom (or an ensemble of \mathcal{N} non-interacting bosons) being confined by a single-mode unidirectional ring cavity, whose cavity mode together with

an additional coherent laser beam form a pair of Raman beams that flips atomic transition between $|\uparrow\rangle$ and $|\downarrow\rangle$ while transferring recoil momentum of $\pm 2\hbar q_r \hat{z}$ from and/or to photon field. Hence, the so-realized effective coupling between atom's external and internal degrees of freedom is generated by the quantized light field, which is affected by atomic dynamics in return. In this sense, the *cavity-assisted* SOC becomes *dynamic*. We show that, at mean field level, the dynamic SOC dramatically modifies the atomic dispersion relation, in particular, with emergence of a loop structure under certain circumstances. We systematically characterize dispersion relation of atomic state and photon number, both as a function of atom's quasi-momentum. For given cavity parameters, we found with increasing Raman coupling strength Ω , dispersion curve changes from double minima to gapped single minimum, looped structure, and gapless single minimum in sequence. Furthermore, we carry out the full quantum mechanical treatment by solving master equations of density operators, and find excellent agreement by comparing averaged photon number with mean field results. The two distinctively different approaches give us an unified understanding of the atom-light effective non-linearity and induced dynamical instability in this system.

The article is organized as the following: After briefly reviewing key ideas of our previous work and semi-classical mean field approach in Sec. 2, we develop the full quantum mechanical formalism to the physical system of interest in Sec. 3 and discuss about the intimate correspondence between the two in Sec. 4, and finally conclude in Sec. 5.

2. Model Setup and Semi-classical Mean Field Formalism

We follow the effective model Hamiltonian proposed in [36],

$$\begin{aligned} \mathcal{H}_{\text{eff}} = & \sum_{\sigma} \int d\mathbf{r} \left[\psi_{\sigma}^{\dagger}(\mathbf{r}) \left(\frac{\hat{\mathbf{k}}^2 + 2\alpha q_r k_z}{2m} + \alpha \tilde{\delta} \right) \psi_{\sigma}(\mathbf{r}) \right] + \frac{\Omega}{2} \int d\mathbf{r} \left[\psi_{\uparrow}^{\dagger}(\mathbf{r}) \psi_{\downarrow}(\mathbf{r}) c + h.c. \right] \\ & + i\varepsilon_p (c^{\dagger} - c) - \delta_c c^{\dagger} c - i\kappa c^{\dagger} c, \end{aligned} \quad (1)$$

where $\psi_{\sigma}(\mathbf{r})$ ($\sigma = \uparrow, \downarrow$) is the atomic operator after gauge transformation in rotating frame at pump frequency ω_p . $\alpha = \pm 1$ for $\sigma = \uparrow, \downarrow$, respectively. q_r denotes recoil momentum, $\tilde{\delta}$ represents the two-photon Raman detuning, ε_p refers to pumping rate, and δ_c is the cavity-pump detuning. Ω describes the atom-photon coupling strength, however, the entire Raman coupling term $\frac{\Omega}{2} \int d\mathbf{r} e^{+2ik_r z} \Psi_{\uparrow}^{\dagger}(\mathbf{r}) \Psi_{\downarrow}(\mathbf{r}) \tilde{c} e^{+i\omega_R t}$ together with its hermitian conjugate describe cavity-assisted two-photon Raman transition processes, where cavity photon amplitude of \tilde{c} or \tilde{c}^{\dagger} is explicitly taken into consideration. It is this coupling that renders the resulting SOC *dynamic*. Furthermore, in the semi-classical approach, we have treated the leakage of cavity photon phenomenologically by introducing a cavity decay rate κ .

From the Hamiltonian (1), one can easily obtain the EOM in Heisenberg picture. To make some progress, we adopt a mean-field approximation by replacing the operators by their respective expectation values: $c \rightarrow \langle c \rangle$, $\psi_{\sigma}(\mathbf{r}) \rightarrow \langle \psi_{\sigma}(\mathbf{r}) \rangle \equiv \varphi_{\sigma}(\mathbf{r})$. The mean-field approximation is justified by assuming small quantum fluctuations of both operators c and $\psi_{\sigma}(\mathbf{r})$. Assuming spatial homogeneity, we further take the plane-wave ansatz for the atomic modes $\varphi_{\sigma}(\mathbf{r}) = e^{i\mathbf{k}\cdot\mathbf{r}} \varphi_{\sigma}$ with the normalization condition $|\varphi_{\uparrow}|^2 + |\varphi_{\downarrow}|^2 = \mathcal{N}$. The steady-state solution for the photon field is obtained by taking the time derivative

of the photon field to be zero. This is known as adiabatic elimination, which essentially assumes cavity photon can always follow atom's instantaneous eigenstates, typically valid for current high-Q cavity experiments. After some algebra, we have the coupled nonlinear time-dependent equations for the two spin components,

$$i\dot{\varphi}_{\uparrow} = \left(\frac{\mathbf{k}^2}{2m} + q_r k_z + \tilde{\delta} \right) \varphi_{\uparrow} + \frac{\Omega}{2} \frac{\varepsilon_p - \frac{i\Omega}{2} \mathcal{N} \varphi_{\downarrow}^* \varphi_{\uparrow}}{\kappa - i\delta_c} \varphi_{\downarrow}, \quad (2)$$

$$i\dot{\varphi}_{\downarrow} = \left(\frac{\mathbf{k}^2}{2m} - q_r k_z - \tilde{\delta} \right) \varphi_{\downarrow} + \frac{\Omega}{2} \frac{\varepsilon_p + \frac{i\Omega}{2} \mathcal{N} \varphi_{\uparrow}^* \varphi_{\downarrow}}{\kappa + i\delta_c} \varphi_{\uparrow}. \quad (3)$$

For a given atomic quasi-momentum \mathbf{k} , we define eigenstate and eigenenergy as the solution of the time-independent version of Eqs. (2) and (3), by replacing $i(\partial/\partial t)$ with $\epsilon(\mathbf{k})$. After some lengthy nonetheless straightforward algebra, we find that $\epsilon(\mathbf{k})$ obeys a quartic equation (we consider $\mathcal{N} = 1$ hereafter):

$$4\epsilon^4 + B\epsilon^3 + C\epsilon^2 + D\epsilon + E = 0, \quad (4)$$

where detailed derivations and coefficients are better elaborated in the Supplementary Material of [36].

[Rewrite it, simplify it and highlight it.] In principle, the quartic equation (4) can be solved analytically, but the expressions too cumbersome to give any physical insights. We plot the typical behavior of the dispersion relation $\epsilon(k_z)$ vs k_z for $\tilde{\delta} = 0$ in Fig. 1. Note that we always take $k_x = k_y = 0$, as the SOC only occurs along the z -axis. A maximum of four real roots are allowed by Eq. (4). As we will show, in such regimes, a loop structure develops in the dispersion curve. As shown in Fig. 1, for $\delta_c = 0$ (i.e., the pump field is resonant with the cavity), we always have two dispersion branches. The two branches are gapped when the atom-photon coupling strength Ω is small and touch each other at $k_z = 0$ when Ω exceeds a critical value. For $\delta_c \neq 0$, we again have two gapped branches at small Ω . As Ω is increased beyond a critical value, a loop appears near $k_z = 0$ in either the upper or the lower branch depending on the sign of δ_c . The loop increases in size as Ω increases and finally touches the other branch and dissolves when Ω reaches a second critical value. Note that such a dispersion relation is markedly different from that without the cavity, in which case one always obtains two gapped branches. The dispersion curves for finite $\tilde{\delta}$ are qualitatively similar, but in that case the curves are no longer symmetric about $k_z = 0$ and the loop emerges at finite k_z .

[Rewrite it, simplify it and highlight it. – also provide discussions on double minimum degeneracy conditions. We should have four regimes in total.] We can gain some insights about the general structure of the dispersion curve, and particularly the appearance and disappearance of the loop, by examining the quartic equation (4) for $k_z = 0$ and $\tilde{\delta} = 0$. Under these conditions, Eq. (4) is simplified to:

$$\epsilon^2(4\epsilon^2 - 2w\epsilon + |v|^2 - 4|u|^2) = 0, \quad (5)$$

with the constraint that the root $\epsilon = 0$ is only valid for $\Omega \geq 4\epsilon_p$ (For $\Omega < 4\epsilon_p$, the solution $\epsilon = 0$ corresponds to trivial state with $\varphi_{\uparrow} = \varphi_{\downarrow} = 0$). Here the coefficients w , u and v are defined in the Supplementary Material of [36]. Simple analysis shows that there are four regimes. First, when $0 < \Omega < \text{SOME VALUE HERE} \equiv \Omega_c^{(0)}$, Eq. (5) has two real roots with degenerate lowest eigenenergy (perhaps some value here as well?). When $\Omega_c^{(0)} < \Omega < 4\epsilon_p \equiv \Omega_c^{(1)}$, Eq. (5) has two real roots, one positive and one negative. This corresponds to the two gapped branches for small Ω in the top row

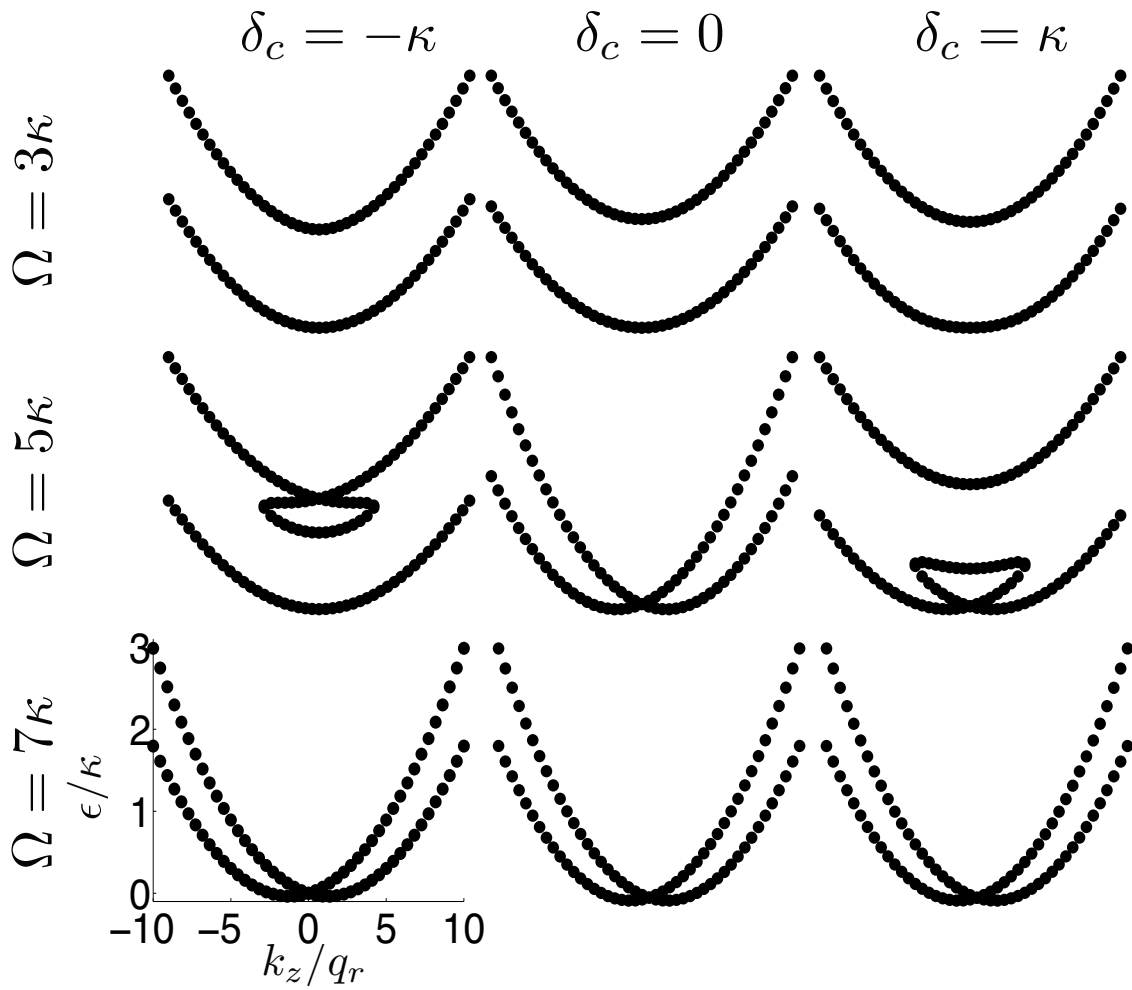


Figure 1. TO BE UPDATED WITH THE ADDITIONAL DOUBLE MINIMUM PLOTS.

Eigenenergy ϵ as a function of quasi-momentum. We set $\tilde{\delta} = 0$ and $\varepsilon_p = \kappa$. For nonzero δ_c , a loop structure forms when $\Omega_c^{(1)} < \Omega < \Omega_c^{(2)}$. For $\delta_c = \pm\kappa$, $\Omega_c^{(1)} = 4\varepsilon_p$ and $\Omega_c^{(2)} = 4\sqrt{2}\varepsilon_p$. Throughout our calculation, we take κ and $\sqrt{2m\kappa}$ to be the units for energy and momentum, respectively. A typical value for κ is $2\pi \times 1$ MHz, and we choose $q_r = 0.22$ in our units.

of Fig. 1. Second, when $\Omega_c^{(1)} \leq \Omega \leq 4\epsilon_p \sqrt{1 + (\delta_c/\kappa)^2} \equiv \Omega_c^{(2)}$, Eq. (5) has four real roots — two degenerate roots at $\epsilon = 0$ and two additional roots with the same sign. This corresponds to the looped regime in the middle row of Fig. 1. Finally when $\Omega > \Omega_c^{(2)}$, only the two degenerate roots at $\epsilon = 0$ exist, which correspond to the gapless regime represented by the bottom row in Fig. 1. Note that for $\delta_c = 0$, we have $\Omega_c^{(1)} = \Omega_c^{(2)} = 4\epsilon_p$, and the loop never develops, nonetheless degeneracy condition still holds as bla bla bla and bla.

[Rewrite it, simplify it and highlight it.] The emergence of the loop structure is a distinctive nonlinear feature of the system. We remark that similar loop structures or the associated hysteretic phenomena have been found in other nonlinear systems [?]. The nonlinearity may originate from the mean-field density-density interaction [?] or from the cavity-induced feedback between atoms and photons [?]. The case studied here corresponds to the latter situation. However, in previous studies of “ultracold atom + cavity” systems [?], the interaction between the cavity photons and atoms is dispersive, and so it does not induce SOC directly. As we will show below, the system studied here possesses very different dynamical and stability properties.

3. Master Equation Approach: Full Quantum Mechanical Treatment

Semi-classical mean field approach gives an intuitive picture of understanding the atom-light interaction, as we have shown above. However, it ignores quantum fluctuations of both operator c and $\psi_\sigma(\mathbf{r})$. A more stringent approach is given by solving quantum master equation, which is especially useful to study few cavity photon scenario. The quantum master equations, in a nutshell, are differential equations for the entire density matrix, including contributions from off-diagonal elements which represents quantum coherence as a characteristic quantum mechanical signature. Master equation is generally considered to be more general than the Schrödinger equation, since it uses the density operator instead of a specific state vector and can therefore give statistical as well as quantum mechanical information.

Instead of treating the leakage of cavity photon phenomenologically in Eq. (1), we model the dissipation process by Liouvillian terms \mathcal{L} appearing in the Lindblad master equation for the atom-field density operator, i.e.,

$$\dot{\rho} = \frac{1}{i\hbar} [H_{\text{eff}}, \rho] + \mathcal{L}\rho. \quad (6)$$

where H_{eff} is the same as \mathcal{H}_{eff} in Eq. (1) by dropping the last term of $-i\kappa c^\dagger c$. Cavity loss of photon is taken as the standard form of Lindblad superoperator [37,38],

$$\mathcal{L}\rho = \kappa(2c\rho c^\dagger - c^\dagger c\rho - \rho c^\dagger c). \quad (7)$$

Again, due to space homogeneity, we decouple momentum eigenstates by taking the plane-wave ansatz for the atomic modes $\varphi_\sigma(\mathbf{r}) = e^{i\mathbf{k}\cdot\mathbf{r}}\varphi_\sigma$. Thereon, we are granted to work with the Hilbert subspace of a given momentum value \mathbf{k} , where we write the commutator explicitly as,

$$\begin{aligned} [H_{\text{eff}}(\mathbf{k}), \rho] &= \left(\frac{\mathbf{k}^2}{2m} + \frac{q_r k_z}{m} + \tilde{\delta} \right) (\varphi_\uparrow^\dagger \psi_\uparrow \rho - \rho \varphi_\uparrow^\dagger \psi_\uparrow) + \left(\frac{\mathbf{k}^2}{2m} - \frac{q_r k_z}{m} - \tilde{\delta} \right) (\psi_\downarrow^\dagger \varphi_\downarrow \rho - \rho \psi_\downarrow^\dagger \varphi_\downarrow) \\ &+ \mathcal{N} \frac{\Omega}{2} (\varphi_\uparrow^\dagger \varphi_\downarrow c \rho + c^\dagger \varphi_\downarrow^\dagger \varphi_\uparrow \rho - \rho \varphi_\uparrow^\dagger \varphi_\downarrow c - \rho c^\dagger \varphi_\downarrow^\dagger \varphi_\uparrow) \\ &+ i\epsilon_p (c^\dagger \rho - c\rho - \rho c^\dagger + \rho c) - \delta_c (c^\dagger c\rho - \rho c^\dagger c). \end{aligned} \quad (8)$$

To this end, we choose our basis states as $|n; \sigma\rangle$, $n = 0, 1, 2, \dots, N$ where N is the truncation number of photon inside the cavity and $\sigma = \uparrow, \downarrow$. Our goal is to calculate the entire matrix elements of density operator under this basis states, where we denote $\langle m; \sigma | \rho | n; \sigma' \rangle \equiv \rho_{mn}^{\sigma\sigma'}$. For arbitrary state, after some lengthy algebra, we found,

$$\begin{aligned} \frac{d}{dt} \rho_{mn}^{\sigma\sigma'} = & -i \left(\frac{\mathbf{k}^2}{2m} + \frac{q_r k_z}{m} + \tilde{\delta} \right) (\delta_{\sigma\uparrow} - \delta_{\sigma'\uparrow}) \rho_{mn}^{\sigma\sigma'} - i \left(\frac{\mathbf{k}^2}{2m} - \frac{q_r k_z}{m} - \tilde{\delta} \right) (\delta_{\sigma\downarrow} - \delta_{\sigma'\downarrow}) \rho_{mn}^{\sigma\sigma'} \\ & + \frac{\Omega \mathcal{N}}{2i} (\delta_{\sigma\uparrow} \sqrt{m+1} \rho_{m+1n}^{\bar{\sigma}\sigma'} + \delta_{\sigma\downarrow} \sqrt{m} \rho_{m-1n}^{\bar{\sigma}\sigma'} - \delta_{\sigma'\uparrow} \sqrt{n+1} \rho_{mn+1}^{\sigma\bar{\sigma}'} - \delta_{\sigma'\downarrow} \sqrt{n} \rho_{mn-1}^{\sigma\bar{\sigma}'}) \\ & + \varepsilon_p \left(\sqrt{m} \rho_{m-1n}^{\sigma\sigma'} - \sqrt{m+1} \rho_{m+1n}^{\sigma\sigma'} + \sqrt{n} \rho_{mn-1}^{\sigma\sigma'} - \sqrt{n+1} \rho_{mn+1}^{\sigma\sigma'} \right) \\ & + i\delta_c (m-n) \rho_{mn}^{\sigma\sigma'} + \kappa \left(2\sqrt{m+1} \sqrt{n+1} \rho_{m+1n+1}^{\sigma\sigma'} - (m+n) \rho_{mn}^{\sigma\sigma'} \right) \end{aligned} \quad (9)$$

where $\bar{\sigma}$ represents the flip-spin value, i.e. $\bar{\uparrow} = \downarrow$ and $\bar{\downarrow} = \uparrow$. Since we have finite truncation number N , we shall ignore terms involving $|N+1; \sigma\rangle$ or $|-1; \sigma\rangle$ generated by photon creation or annihilation operators.

With Eq. 9, we can of course study dynamical evolution of density operator ρ for a given initial state. For instance, we can initiate the system with a pure state $|0; \uparrow\rangle$, construct density operator $\rho = |0; \uparrow\rangle\langle 0; \uparrow|$, and let it evolve according to Eq. 9. Although at $t = 0$ we have $\text{Tr}[\rho^2] = 1$, at later time, we will always have $\text{Tr}[\rho^2] < 1$ because cavity decay term renders the system into mixed states. The fate of time evolution gives the steady state solution, which can also be obtained by solving a set of linear equations after taking the RHS of Eq. 9 to zero.

From the steady state solution of density operator, we can compute expectation value of any observable operator \hat{O} by taking the product trace, i.e. $\langle \hat{O} \rangle = \text{Tr}[\rho \hat{O}]$. For instance, we compute photon number as $\langle n \rangle = \text{Tr}[\rho n] = \rho_{nn}^{\uparrow\uparrow} + \rho_{nn}^{\downarrow\downarrow}$ and photon number fluctuation $\frac{\langle (\Delta n)^2 \rangle}{\langle n \rangle} = \frac{\langle n^2 \rangle - \langle n \rangle^2}{\langle n \rangle}$, where $\langle m; \sigma | c^\dagger c c^\dagger c | n; \sigma' \rangle = n^2 \delta_{mn} \delta_{\sigma\sigma'}$. If $\frac{\langle (\Delta n)^2 \rangle}{\langle n \rangle} > 1$, it is super-Poissonian; if $\frac{\langle (\Delta n)^2 \rangle}{\langle n \rangle} = 1$, it is Poissonian; if $\frac{\langle (\Delta n)^2 \rangle}{\langle n \rangle} < 1$, it is sub-Poissonian. Also, the probability of finding n photon is defined as $p(n) = \langle n | \hat{\rho}_{\text{photon}} | n \rangle$ where $\hat{\rho}_{\text{photon}}$ is the reduced density matrix for photon by tracing over atomic degrees of freedom in total density operator, i.e. $\rho_{\text{photon}} = \text{Tr}_{\text{atom}}[\rho]$. For coherent light, $p_{\text{coh}}(n) = \frac{\langle n \rangle^n}{n!} e^{-\langle n \rangle}$; and for thermal light, $p_{\text{th}}(n) = \frac{1}{1+\langle n \rangle} \left(\frac{\langle n \rangle}{1+\langle n \rangle} \right)^n$. We have found small pumping rate ε_p gives better fit of $p(n)$ to $p_{\text{th}}(n)$ and for large value of ε_p , $p(n)$ is closer to $p_{\text{coh}}(n)$.

Negativity for mixed state is defined as $\mathcal{N}(\rho) = \frac{\|\rho^{T_{\text{atom}}}\|_1 - 1}{2} = \frac{(\sum \text{eig}[\rho^{T_{\text{atom}}}] - 1)}{2} = \sum_i \frac{|\lambda_i| - \lambda_i}{2}$ where λ_i are all the eigenvalues of $\rho^{T_{\text{atom}}}$. Namely, negativity is the absolute sum of negative eigenvalues of $\rho^{T_{\text{atom}}}$, which vanishes for unentangled states. Also, $\rho^{T_{\text{atom}}}$ stands for partial transpose of density matrix with respect to atom party, $\rho^{T_{\text{atom}}} = \begin{pmatrix} [\rho_{mn}^{\uparrow\uparrow}]^T & [\rho_{mn}^{\uparrow\downarrow}]^T \\ [\rho_{mn}^{\downarrow\uparrow}]^T & [\rho_{mn}^{\downarrow\downarrow}]^T \end{pmatrix}$.

4. Results and Discussions

5. Conclusions

Acknowledgments

Author Contributions

H.P. conceived the idea of the project, L.D. and C. Z. explored the theoretical and numerical aspects of the physics. All authors contributed to writing and revising the manuscript and participated in the discussions about this work.

Conflicts of Interest

The authors declare no conflict of interest.

References

1. Anderson, M. H., J. R. Ensher, M. R. Matthews, C. E. Wieman, and E. A. Cornell, *Science* **1995**, 269, 198.
2. Bradley, C. C., C. A. Sackett, J. J. Tollett, and R. G. Hulet, *Phys. Rev. Lett.* **1995**, 75, 1687.
3. Davis, K. B., M.-O. Mewes, M. R. Andrews, N. J. van Druten, D. S. Durfee, D. M. Kurn, and W. Ketterle, *Phys. Rev. Lett.* **1995**, 75, 3969.
4. DeMarco, B., and D. D. Jin, *Science* **1999**, 285, 1703.
5. Truscott, A., K. Strecker, W. McAlexander, G. Partridge, and R. G. Hulet, *Science* **2001**, 291, 2570.
6. Schreck, F., L. Khaykovich, K. L. Corwin, G. Ferrari, T. Bourdel, J. Cubizolles, and C. Salomon, *Phys. Rev. Lett.* **2001** 87, 080403.
7. Bloch, I., *Nature Physics* **2005**, 1 23.
8. Bloch I. and M. Greiner, *Adv. At. Mol. Opt. Phys.* **2005**, 52 1.
9. Jaksch, D., C. Bruder, J. I. Cirac, C. W. Gardiner, and P. Zoller, *Phys. Rev. Lett.* **1998**, 81, 3108.
10. W. Zwerger, *J. Opt. B* **2003**, 5, 9.
11. Chevy, F.; Salomon, C. Thermodynamics of Fermi Gases. In *The BCS-BEC Crossover and the Unitary Fermi Gas*; Zwerger, W.; Springer: Lecture Notes in Physics, Vol. 836, 2012; pp. 407-446.
12. Ketterle, W.; Zwierlein, M. W., Making, probing and understanding ultracold Fermi gases. In *Ultra-cold Fermi Gases*; Inguscio, M., Ketterle, W., Salomon, C.; IOP Press: Proceedings of the International School of Physics “Enrico Fermi”, 2007; pp.95-287.
13. Brennecke, F., Donner, T., Ritter, S., Bourdel, T., Kohl, M., and Esslinger, T., *Nature* **2007**, 450 268.
14. Colombe, Y., Steinmetz, T., Dubois, G., Linke, F., Hunger, D. and Reichel, J. *Nature* **2007**, 450 272.
15. Slama, S., Bux, S., Krenz, G., Zimmermann, C. and Courteille, Ph. W. *Phys. Rev. Lett.* **2007**, 98 053603.
16. J. M. Raimond, M. Brune, and S. Haroche, *Rev. Mod. Phys.* **2001**, 73, 565.
17. R. Miller, T. E. Northup, K. M. Birnbaum, A. Boca, A. D. Boozer, and H. J. Kimble, *J. Phys. B* **2005**, 38, S551.
18. H. Walther, B. T. H. Varcoe, B.-G. Englert, and T. Becker, *Rep. Prog. Phys.* **2006**, 69, 1325.
19. F. Brennecke, T. Donner, S. Ritter, T. Bourdel, M. Köhl, and T. Esslinger, *Nature (London)* **2007**, 450, 268.

20. Y. Colombe, T. Steinmetz, G. Dubois, F. Linke, D. Hunger, and J. Reichel, *Nature* (London) **2007**, 450, 272.
21. S. Slama, S. Bux, G. Krenz, C. Zimmermann, and Ph. W. Courteille, *Phys. Rev. Lett.* **2007**, 98, 053603.
22. D. Schmidt, H. Tomczyk, S. Slama, and C. Zimmermann, arXiv:1311.2156 (2013).
23. S. Gupta, K. L. Moore, K. W. Murch, and D. M. Stamper-Kurn, *Phys. Rev. Lett.* **2007**, 99, 213601.
24. M. Lewenstein, A. Sanpera, V. Ahufinger, B. Damski, A. Sen De, and U. Sen, *Adv. Phys.* **2007**, 56, 243.
25. I. B. Mekhov and H. Ritsch, *J. Phys. B* **2012**, 45, 102001.
26. Y.-J. Lin, K. Jimenez-Garcia, and I. B. Spielman, *Nature* (London) **2011**, 471, 83.
27. Y.-J. Lin, R. L. Compton, K. Jimenez-Garcia, W. D. Phillips, J. V. Porto, and I. B. Spielman, *Nat. Phys.* **2011**, 7, 531.
28. P. Wang, Z.-Q. Yu, Z. Fu, J. Miao, L. Huang, S. Chai, H. Zhai, and J. Zhang, *Phys. Rev. Lett.* **2012**, 109, 095301.
29. L. W. Cheuk, A. T. Sommer, Z. Hadzibabic, T. Yefsah, W. S. Bakr, and M. W. Zwierlein, *Phys. Rev. Lett.* **2012**, 109, 095302.
30. V Galitski, I B Spielman, *Nature* **2013**, 494 7435.
31. Hasan, M. Z., Kane, C. L. *Rev. Mod. Phys.* **2010**, 82 3045–3067.
32. Sau, J. D., Lutchyn, R. M., Tewari, S. and Sarma, Das, S. *Phys. Rev. Lett.* **2010**, 104 040502.
33. Burkov, A. A. and Balents, L., *Phys. Rev. Lett.* **2011**, 107 127205.
34. Sinova, J., Cilcer, D., Niu, Q., Sinitsyn, N., Jungwirth, T., and MacDonald, A., *Phys. Rev. Lett.* **2004**, 92 126603.
35. Kato, Y. K., Myers, R. C., Gossard, A. C. and Awschalom, D. D., *Science* **2004**, 306 1910–1913.
36. Lin Dong, Lu Zhou, Biao Wu, B. Ramachandhran, and Han Pu, *Phys. Rev. A* **2014** 89, 011602(R).
37. Kossakowski, A. *Rep. Math. Phys.* **1972**, 3 (4): 247.
38. Lindblad, G. *Commun. Math. Phys.* **1976**, 48 (2): 119.

© 2015 by the authors; licensee MDPI, Basel, Switzerland. This article is an open access article distributed under the terms and conditions of the Creative Commons Attribution license (<http://creativecommons.org/licenses/by/4.0/>).